

ELM Pacing with 3D Magnetic Perturbations in NSTX

J.M. Canik¹, R. Maingi¹, A.C. Sontag¹, J.-W. Ahn¹, R.E. Bell², D.A. Gates², S.P. Gerhardt², H.W. Kugel², B.P. LeBlanc², J.E. Menard², S.F. Paul², S.A. Sabbagh³, V.A. Soukhanovskii⁴

¹ Oak Ridge National Laboratory, Oak Ridge, TN, USA

² Princeton Plasma Physics Laboratory, Princeton University, Princeton, NJ, USA

³ Columbia University, New York, NY, USA

⁴ Lawrence Livermore National Laboratory, Livermore, CA, USA

The energy expelled by edge localized modes (ELMs) poses a serious threat to the lifetime of plasma facing components (PFCs) in future large devices such as ITER, making the control of ELM size critically important. However, ELMs also expel particles and thus have the beneficial effect of aiding density and impurity control. The difficulty of controlling particle inventory during ELM-free H-modes has been evident in recent experiments in the National Spherical Torus Experiment (NSTX), where lithium coatings have been applied to the PFCs to reduce particle recycling¹. These coatings improve energy confinement^{2,3}, but also result in the elimination of ELMs^{4,5}, and so suffer from strong accumulation of carbon and metallic impurities⁶ along with a secular rise in the electron density. Here we describe efforts to mitigate the particle accumulation in such discharges by inducing ELMs using externally applied non-axisymmetric magnetic perturbations. Although this ELM pacemaking technique is primarily used for impurity control in NSTX, this method also may be used to control the ELM frequency and size.

The destabilization of ELMs by applied $n=3$ fields in NSTX was initially studied using boronized carbon PFCs without lithium coatings^{7,8}. Under these conditions, ELMs of many types are routinely observed, including very small Type-V ELMs⁹. When the 3D field was turned on during an ELM-free or small-ELM phase of the discharge, it was observed that large ELMs began within ~ 50 ms. Edge profile measurements showed that, in the period between the 3D field turn-on and ELM onset, the pedestal electron temperature increased, while the density and ion temperature remained relatively unchanged. The net result was a $\sim 30\%$ increase in the total peak pressure gradient in the pedestal. This increase was sufficient to destabilize low- n edge modes⁷, according to calculations using the PEST MHD stability code¹⁰; PEST indicates stability to these modes in the case prior to the $n=3$ field application.

The destabilization of ELMs by 3D fields has also been observed in discharges where lithium coatings have been used, eliminating all types of natural ELMs. In this case, the

modification to the pedestal profiles that occurs following the $n=3$ field application prior to ELM onset differs from discharges without lithium coatings. Both the electron density and temperature are modified (figure 1), showing a reduction in the density “ear” at the top of the pedestal following the 3D field application¹¹, and a flattening of the temperature in the same

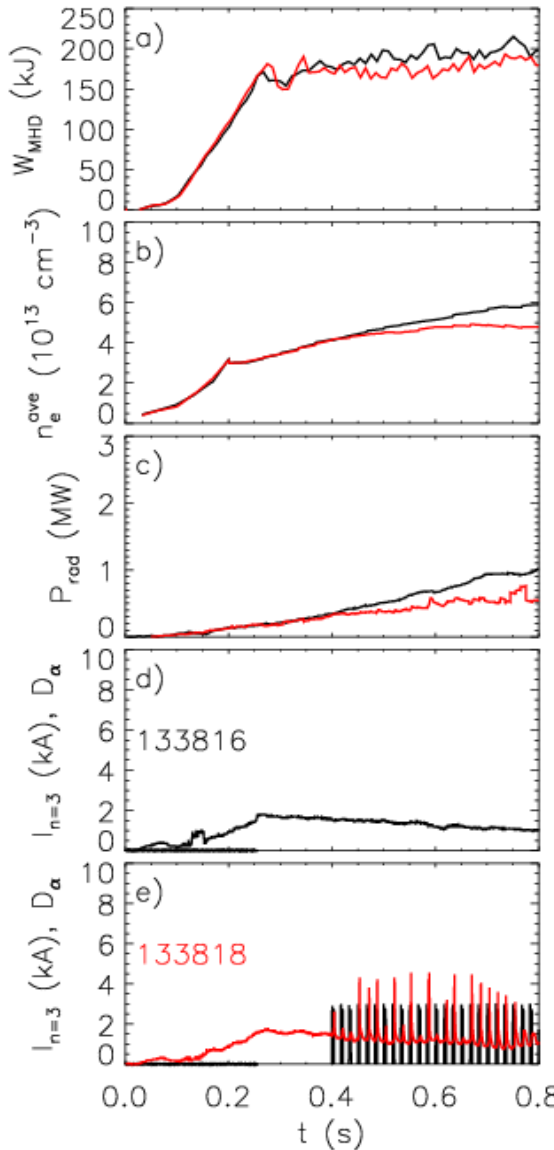


Figure 2: a) Stored energy, b) line-averaged density, c) radiated power and d-e) current in the $n=3$ coil set and divertor D_α emission without (black) and with (red) $n=3$ induced ELMs

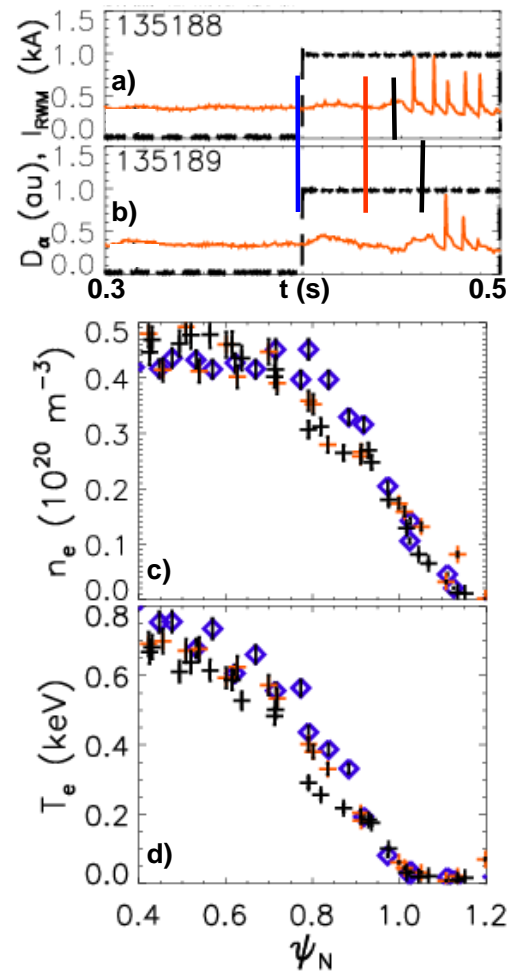


Figure 1: a,b) Time traces of D_α (red) and applied $n=3$ field (dashed black), with vertical bars (blue, red black) indicating timing of profile measurements. Profiles of the pedestal electron c) density and d) temperature before (blue) and after (red and black) $n=3$ field application.

region. However, in the steep gradient region outside of $\psi_N \sim 0.9$, the profiles are not substantially modified by the $n=3$ field, leaving the cause of the change in ELM stability unknown under these conditions.

The destabilizing effect of 3D fields has been used to trigger ELMs at will during discharges with lithium coatings, as a pacing technique for control of impurity buildup by restoring the particle “flushing” from ELMs^{7,8}. This technique has been successful in reducing impurity radiation and slowing

the density rise during these discharges. Through optimization of the triggering waveform, periods of quasi-stationary conditions have been produced in the line-integrated electron density and total radiated power¹², as shown in Figure 2. In addition, ELM-pacing has been combined with the partial replacement of gas fuelling from a slow valve located on the center column with a fast supersonic gas injector¹³ to enhance the density control and help produce these quasi-stationary periods. However, during these phases the profiles continue to evolve: the edge density and radiation decrease in time, while the core values continue to increase¹². Core impurity control using e.g. central electron heating¹⁴ will soon be tested to mitigate this central accumulation.

Aside from impurity control, ELM pacing using 3D field pulses provides a means for controlling the ELM frequency, and possibly the ELM size. Indeed, the experiments have shown that increasing the triggering (and hence ELM) frequency reduces the fraction of plasma stored energy that is expelled by an ELM, although the reduction is substantially weaker than an inverse scaling with frequency¹². Figure 3 shows the reduction in ELM size with frequency as measured by a fast IR camera¹⁵; although the scaling is valid, the absolute energy is uncertain as the presence of lithium films modifies the surface emissivity and film characteristics, which is unaccounted for in the calibrations. It should be noted that these data were taken with a plasma current $I_p=1$ MA; a stronger decrease of ELM size (based on fast equilibrium reconstructions) with frequency has been observed at $I_p=800$ kA¹².

It was recently observed that during $n=3$ field pulses that fail to trigger an ELM (due to the pulse being either too brief or too low in amplitude), an occasional slow, small-amplitude rise is observed in the divertor D_α emission. Based on the assumption that this represents an enhancement of particle transport, experiments were performed to test if $n=3$ pulses below the threshold for ELM triggering could be used for impurity control, avoiding large ELMs. By tailoring the amplitude and durations of the 3D field pulses, trains of many pulses were achieved that successfully produced brief increases in D_α while avoiding large ELMs. The response to the applied field is evident on several diagnostics, including fast D_α

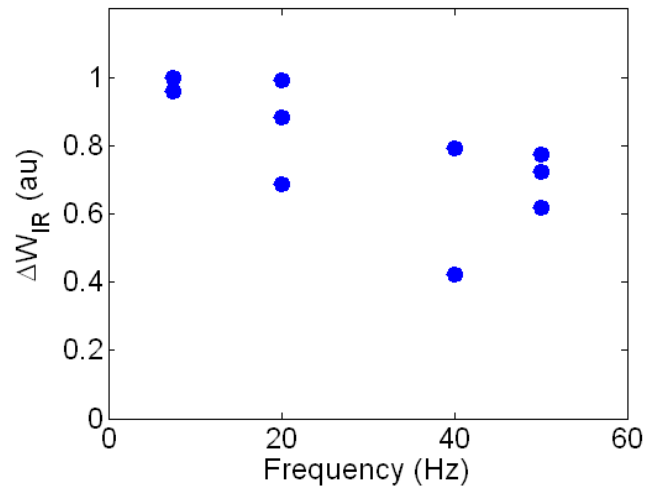


Figure 3: Energy expelled by ELMs vs. triggered ELM frequency, measured by fast IR thermography

and IR cameras as well as soft X-ray detectors, suggesting that the 3D field is triggering an initial instability or change in transport. However, these low-level pulses did not cause sufficient particle expulsion to provide impurity control: the radiated power and carbon content during discharges with these pulse trains was nearly unchanged compared to the control case (figure 4).

While the measured changes during the $n=3$ pulses may give further insight into the impact of 3D fields on plasma behavior, this technique of using sub-threshold $n=3$ pulses without ELMs appears to be ineffective for providing the needed particle control with lithium coated PFCs. To provide this control further optimization of the ELM-pacing technique is being explored, for example in combination with RF heating to mitigate core accumulation, and with ELM triggering via vertical jogs to increase the ELM frequency. One additional approach may be to control the impurity source directly through modification of the divertor conditions¹⁶ to reduce sputtering.

This research was sponsored in part by U.S. Dept. of Energy Contracts DE-AC05-00OR22725, DE-AC02-09CH11466, DE-AC52-07NA27344 and DE-FG02-99ER54524

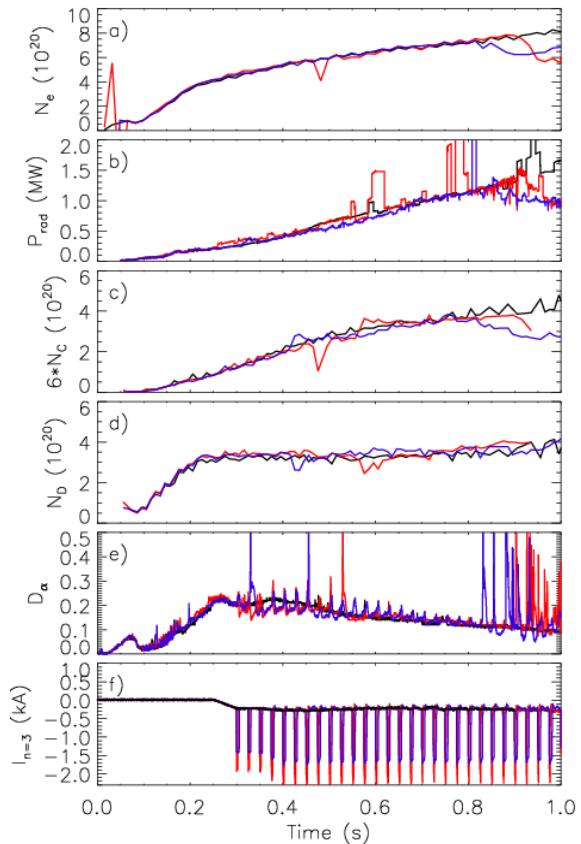


Figure 4: Total a) electron, b) radiated power, c) carbon and d) deuterium inventories, e) $D\alpha$ and f) $n=3$ coil current in a control discharge (black) and with sub-threshold $n=3$ pulses (red and blue).

¹ H.W. Kugel *et al*, Phys. Plasma **15** (2008) 056118.

² M.G. Bell *et al*, Plasma. Phys. Contr. Fusion **51** (2009) 124054.

³ S. Ding *et al*, Plasma Phys. Contr. Fusion **52** (2010) 015001.

⁴ D.K. Mansfield *et al*, J. Nucl. Mat. **390-391** (2009) 764.

⁵ R. Maingi *et al*, Phys. Rev. Lett. **103** (2009) 075001.

⁶ S.F. Paul *et al*, J. Nucl. Mat. **390-391** (2009) 211.

⁷ J.M. Canik *et al*, Phys. Rev. Lett. **104** (2010) 045001.

⁸ J.M. Canik *et al*, Nucl. Fusion **50** (2010) 034012.

⁹ R. Maingi *et al*, Nucl. Fusion **45** (2005) 1066.

¹⁰ R. Grimm *et al*, Methods. Comput. Phys. **16** (1976) 253.

¹¹ J.-W. Ahn *et al*, Nucl. Fusion **50** (2010) 045010.

¹² J.M. Canik *et al*, Nucl. Fusion **50** (2010) 064016.

¹³ V.A. Soukhanovskii *et al*, Rev. Sci. Instrum. **75** (2004) 4320.

¹⁴ O. Gruber *et al*, Nucl. Fusion **49** (2009) 115014.

¹⁵ J.-W. Ahn *et al*, Rev. Sci. Instrum. **81** (2010) 023501.

¹⁶ V.A. Soukhanovskii *et al*, Nucl. Fusion **49** (2009) 095025.